Mechanically Milling with Off-the-Shelf Magnesium Powder to Promote Hydrogen Release from Ammonia Borane

Jun-Hong Luo, Xiang-Dong Kang, and Ping Wang*

Shenyang National Laboratory for Materials Science, Institute of Metal Research, Chinese Academy of Sciences, Shenyang, 110016, China

Received: December 17, 2009; Revised Manuscript Received: March 28, 2010

Mechanically milling with the off-the-shelf magnesium (Mg) powder can dramatically improve the dehydrogenation properties of ammonia borane (AB) on all key aspects: enhancing the dehydrogenation kinetics, reducing the induction period, suppressing the formation of volatile byproduct, and alleviating the sample foaming. The postmilled AB/0.5Mg sample can release 8.2 wt % of hydrogen at 100 °C within 4 h and deliver >2.5 equiv of hydrogen in AB upon elevating the dehydrogenation temperature to 300 °C, giving a material-based hydrogen capacity of 12 wt %. Additionally, the dehydrogenation reaction of the AB/0.5Mg sample becomes significantly less exothermic than that of pristine AB, and remarkably, the third dehydrogenation step is tailored to be endothermic. Combination of phase/structure/chemical state analyses suggest that a considerable amount of Mg participates in the dehydrogenation process, resulting in the formation of Mg−N−B−H product(s).

Introduction

On-board hydrogen storage is a major technical barrier to the widespread use of hydrogen as a transportation fuel. Compared with pressurized tanks and cryogenic liquid hydrogen, material-based solid-state hydrogen storage holds greater promise to provide safe and efficient means for on-board hydrogen storage. The past decades have witnessed explosive growth of solid hydrogen storage materials that extend from interstitial metal hydrides to complex anionic hydrides, from nanostructured carbon to novel metal−organic framework materials. Nevertheless, none of these identified material systems can meet the principal technical requirements for on-board hydrogen sources.[1−3] Recently, ammonia borane (NH_3BH_3, AB) has garnered considerable interest as a potential hydrogen storage medium, owing to its combined advantages of high hydrogen content (∼19.6 wt %), moderate thermal stability, and satisfactory air stability.[4−6] However, there are several problems hindering its practical use: (1) the sluggish dehydrogenation kinetics at temperature <100 °C, and the release of its third equivalent of hydrogen requires temperature >500 °C; (2) the concurrent release of volatile byproduct, for example, B_2H_6, *c*-$(NHBH)_3$, which are detrimental to the fuel cell; (3) serious foaming that occurs in the decomposition process complicates engineering design; and (4) lack of energy- and cost-efficient routes for regeneration of AB from the decomposition products.

Several approaches have been recently developed to improve the dehydrogenation properties of AB. The addition of selected transition metal catalysts,[7−10] acids,[11] or ionic liquids[12] can effectively promote the dehydrocoupling reaction of AB under mild conditions. Similarly, adding metal catalysts[13,14] or solid acids[15] enables vigorous H_2 release from the aqueous solutions of AB at room temperature. Although these approaches have proven to be effective in improving both the rate and extent of H_2 release from AB, the usage of aqueous or nonaqueous solutions makes the hydrogen density of the systems unacceptably low for practical applications. Likewise, the strategy of confinement of AB using nanostructured scaffolds[16−18] or poly(methyl acrylate) (PMA)[19] also suffers from serious capacity loss. Quite recently, chemical modification has been established as a new promising approach for improving the dehydrogenation properties of AB material.[20−25] Several metal-substituted derivatives of AB, for example, $LiNH_2BH_3$ (LAB),[20,21] $NaNH_2BH_3$ (SAB),[20,22] $Ca(NH_2BH_3)_2$,[23,24] and $Sr(NH_2BH_3)_2$,[25] have been successfully synthesized by mechanochemical or solution methods. Compared with pristine AB, the alkali or alkaline earth metal amidoboranes exhibit enhanced dehydrogenation kinetics and thereby higher deliverable hydrogen capacity at moderate temperatures, suppressed evolution of volatile B-containing byproduct, and reduced reaction exothermicity. Additionally, it was recently found that mechanically milling with MgH_2 can also dramatically improve the dehydrogenation properties of AB.[26] Because no experimental evidence has been obtained to show the formation of $Mg(NH_2BH_3)_2$ in the AB/MgH_2 system, this finding exemplified a novel solid-phase activation approach for promoting hydrogen release from AB. In comparison with the metal cation substitution strategy, the latter approach is more flexible in choosing the solid promoter and thereby potentially allows for more tunable hydrogen storage properties of AB.[26,27]

In our study following the solid-phase activation approach, we found that the commercial Mg powder is also an effective promoter for AB material. The postmilled AB/0.5Mg sample showed 8.2 wt % hydrogen release from AB at 100 °C with no detectable amount of volatile byproduct; elevating the operation temperature to 300 °C enables 16.8 wt % hydrogen release from AB, giving a material-based hydrogen capacity of 12 wt %. Furthermore, mechanically milling with Mg powder was found to suppress sample foaming effectively and to tailor the thermochemical property of AB favorably. We herein report these experimental results as well as the preliminary mechanistic study of the promoting effect of Mg additive.

* To whom correspondence should be addressed. E-mail: pingwang@imr.ac.cn. Fax: +86 24 2389 1320. Tel: +86 24 2397 1622.

10.1021/jp911931t
Published on Web 05/18/2010

Experimental Section

AB was synthesized by the reaction of ammonium carbonate and sodium borohydride in tetrahydrofuran solution at 45 °C following the procedure detailed in literature.[28] The purity of the prepared AB (>95%) was verified by XRD measurements, solid state ^{11}B NMR studies, and elemental analyses (Table S1, Supporting Information). Magnesium powder (purity >99%) was purchased from Aldrich and used as received. The AB/xMg powder mixtures in varied molar ratio (x = 0.1 to 1) were mechanically milled under an argon (99.999% purity) atmosphere using a SPEX8000 mill. The ball-to-powder ratio was around 40:1. All sample handlings were carried out in an argon (99.999% purity)-filled glovebox equipped with a circulative purification system, in which the H_2O/O_2 levels were typically <0.1 ppm.

The thermal decomposition behaviors of the pristine AB and the AB/Mg samples were examined by synchronous thermogravimetry/differential scanning calorimetry/mass spectroscopy (TG/DSC/MS, Netzsch 449C Jupiter/QMS 403C) and by volumetric method. In the thermal analyses, we employed the specially designed crucibles made up of stainless steel. In a typical measurement run, the sample with an amount of ~3 mg was heated to 300 °C at a ramping rate of 2 °C/min under a flowing argon (99.999% purity) atmosphere. The isothermal dehydrogenation and temperature-programmed desorption (TPD) measurements (with a typical sample amount of 100 mg) were performed using a carefully calibrated Sievert's type apparatus. Precise pressure measurement was accomplished using a high-precision pressure transducer. Typically, the dehydrogenation measurements were performed under an initial pressure <100 Pa. Other than specified, the H-capacity of the AB/0.5Mg sample was determined on the basis of AB to allow for a property comparison with the pristine AB.

The AB/Mg samples were characterized by Fourier transformation infrared spectroscopy (FTIR, Bruker Tensor 27, 4 cm^{-1} resolution), X-ray diffraction (XRD, Rigaku D/max 2500, Cu Kα radiation), and X-ray photoelectron spectroscopy (XPS, VG ESCALAB 250, Al Kα radiation). All sample handlings were carried out in the argon-filled glovebox, and special measures were taken to minimize H_2O/O_2 contamination during the sample transferring processes. The FTIR spectra were collected using the KBr-pellet method, and the obtained spectra were normalized using OPUS 6.5 software. In the XPS measurements, high-resolution scans of elemental lines were recorded at 50 eV pass energy of the analyzer. Binding energies of all samples were calibrated using the C 1s peak (284.6 eV) of the adventitious carbon as an internal standard. XPS spectra were fitted using a nonlinear least-squares program with a mixed Gaussian−Lorentzian product function provided by XPSPEAK 4.1 software.

Results and Discussion

Study of Dehydrogenation Properties. Mechanically milling with Mg powder can dramatically improve the dehydrogenation properties of AB. A preliminary study found that the overall dehydrogenation property of the AB/xMg samples reached its maximum when the molar ratio x was increased to 0.5 and after the sample was mechanically milled under an argon atmosphere for 2 h. The thus-prepared sample was selected for further detailed property examinations. Figure 1 compares the thermal decomposition behaviors of the AB/0.5Mg and pristine AB samples examined by synchronous TG/DSC/MS. Compared with pristine AB, the AB/0.5Mg sample exhibits a series of remarkable property advantages. First, the dehydrogenation

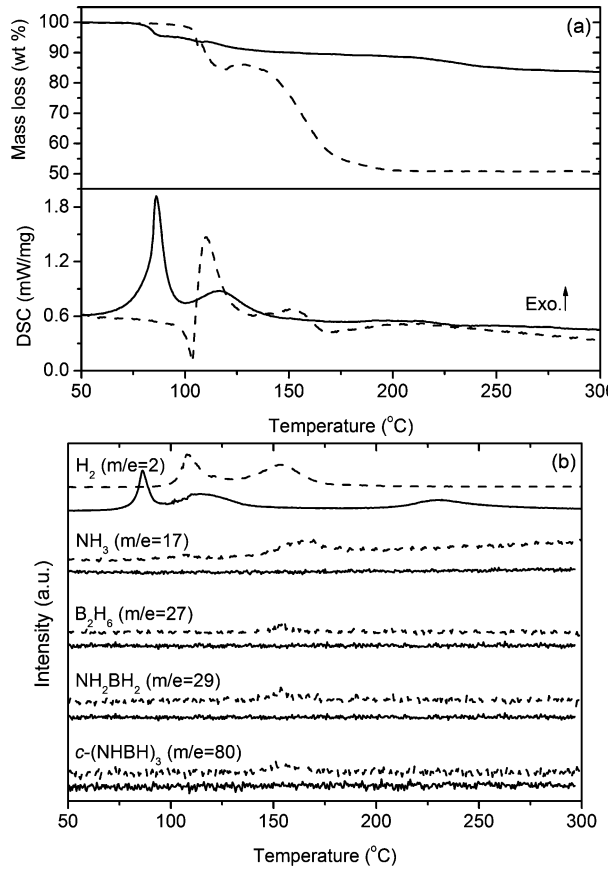

Figure 1. (a) TG/DSC profiles and (b) synchronous MS profiles of m/e = 2 (H_2), 17 (NH_3), 27 (B_2H_6), 29 (NH_2BH_2), and 80 (c-$(NHBH)_3$) of the postmilled AB/0.5Mg and pristine AB samples. The profiles of the AB/0.5Mg sample are presented in solid lines and those of pristine AB are presented in dashed lines.

temperature was significantly lowered with the presence of Mg additive. For pristine AB, following a sharp endothermic melting peak at 103 °C, two exothermic events were observed to center at approximately 110 and 152 °C, which correspond to the first two decomposition steps yielding polymeric amidoboranes ($(NH_2BH_2)_n$, PAB) and polymeric imidoboranes ($(NHBH)_n$, PIB) solid residues, respectively.[29−33] In contrast, dehydrogenation of the AB/0.5Mg sample was initiated at temperature as low as ca. 70 °C, and the rapid release of the first and the second equivalent of H_2 occurred at around 86 and 116 °C, respectively. Notably, careful examination of the MS result found a third H_2 desorption peak at ~232 °C, and according to the synchronous TG result, the desorbed hydrogen amount in the third dehydrogenation step is ~5 wt %. According to the FTIR analysis of the postheated sample (Figure 6), this dehydrogenation step should correspond to the release of the third equivalent H_2 from AB. This is an important finding because pristine AB can only release its third equivalent H_2 at temperature >500 °C.[29,30] To our knowledge, this is the first report of AB releasing its last residual hydrogen at such relatively moderate temperature via thermolysis process. Second, the evolution of volatile byproduct was largely reduced. As shown in Figure 1b, the thermal decomposition of pristine AB involves the concurrent release of considerable amounts of ammonia (NH_3), diborane (B_2H_6), monomeric aminoborane (H_2NBH_2), and borazine (c-$(NHBH)_3$) together with H_2, particularly at the second decomposition step.[31,34,35] This qualitatively accounts for the TG result, which determined a significantly larger weight loss (49 wt %) than the expected value (13 wt %) upon releasing two equivalents

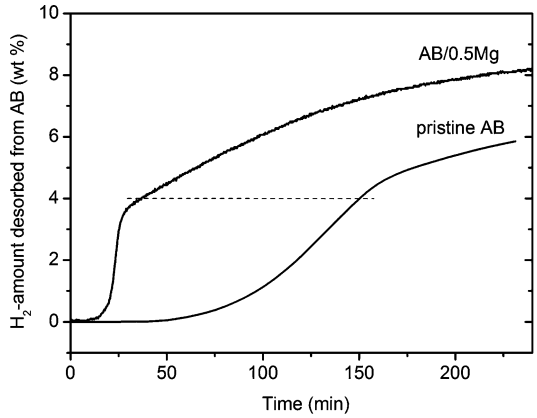

Figure 2. Dehydrogenation kinetics curves of the postmilled AB/0.5Mg sample and pristine AB at 100 °C.

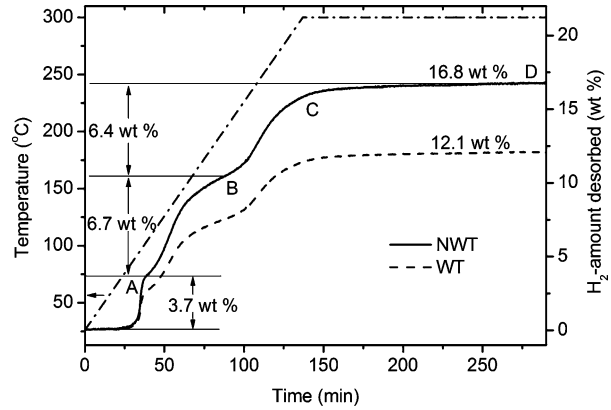

Figure 3. Temperature-programmed desorption profile of the postmilled AB/0.5Mg sample. The hydrogen capacity is calculated on the basis of AB (solid line, NWT) and total sample weight (dash line, WT), respectively. The ramping rate is 2 °C/min.

of H_2 from AB. In contrast, no volatile byproduct can be detected throughout the decomposition process of the AB/0.5Mg sample up to 300 °C within the detection limit of our MS apparatus. Third, the dehydrogenation reaction became significantly less exothermic by adding Mg. According to the combined TG/DSC results, the enthalpy for the release of the first equivalent H_2 from pristine AB was estimated to be ca. 22 kJ/mol H_2, which is in good agreement with the reported values.[31] Whereas for the AB/0.5Mg sample, this value was dramatically reduced to ca. 12 kJ/mol H_2. Similar reduction of reaction enthalpy was also observed in AB/mesoporous silica nanocomposite,[16] LAB,[20,21] and AB/0.5MgH_2[26] materials. From an energetic point of view, the reduced reaction exothermicity should facilitate the subsequent hydride regeneration from the decomposition products. Of particular interest, the third dehydrogenation step of the AB/0.5Mg sample was found to be slightly endothermic, which is indicative of the possibility of partial hydride regeneration via solid−gas reaction. But the preliminary attempt using a condition of 300 °C and 10 MPa H_2 pressure to recharge the solid products that were generated in the third dehydrogenation step failed up to now.

In a general view, Mg shows similar promoting effect to MgH_2 for the hydrogen release from AB.[26] But in terms of alleviating sample foaming in the thermal decomposition process, Mg is better than MgH_2. This is evident from visual examinations of the postheated samples with Mg and MgH_2 additives, respectively. Currently, the mechanism underlying the alleviation of sample foaming remains unclear, but it seems improper to attribute simply the alleviated foaming to solid-phase decomposition[34] because serious foaming was also observed in the AB/MgH_2 material, which exhibits dehydrogenation properties quite similar to those of the present AB/0.5Mg material. In addition, our designed experiment of the AB/Al sample precluded the possibility that the alleviated foaming is correlated to the increased thermoconductivity upon the addition of metal powders.

To gain more insight into the property enhancement arising upon the addition of Mg, we further examined the AB/0.5Mg and pristine AB samples using the volumetric method. Figure 2 compares the isothermal dehydrogenation property of the two samples. (Ignore the error arising upon the incapability of distinguishing volatile byproduct from hydrogen for the pristine AB.) It was found that the addition of Mg results in significantly reduced induction period. Here it should be noted that in our isothermal measurements, data collection was started from the moment of pushing the reactor into the furnace that was preheld at 100 °C. Therefore, the initial short flat sections in the kinetics curves do not reflect appropriately the intrinsic property of the AB/0.5Mg sample but mostly an artifact resulting from the measurement method. The shortened induction period clearly means prompt transient response, which is vital for practical hydrogen storage applications. Similar reduction of induction period was also observed in the AB systems with ionic liquid,[12] diammoniate of diborane (DADB),[36] MgH_2,[26] or transition-metal chlorides[34,35] additives. Aside from the markedly reduced induction period, AB/0.5Mg sample exhibits distinct advantages over pristine AB on both the rate and extent of H_2 release. The pristine AB releases ∼4 wt % of hydrogen within 2.5 h at 100 °C; whereas for the AB/0.5Mg sample, it takes about 0.5 h to release the same amount of hydrogen. Upon extending the reaction time to 4 h, the hydrogen released from AB/0.5Mg sample amounts to ca. 8.2 wt %, which is 2.3 wt % higher than that from pristine AB. After taking the weight of Mg additive into account, the deliverable hydrogen capacity of the AB/0.5Mg sample is ∼6 wt % at 100 °C.

Figure 3 presents the TPD result of the AB/0.5Mg sample, which shows a distinct multistep dehydrogenation feature. At a ramping rate of 2 °C/min, the sample was observed to complete the first and the second dehydrogenation step at approximately 100 and 200 °C (marked by A and B, respectively), yielding ∼3.7 and 6.7 wt % hydrogen, respectively. Upon being further heated to 300 °C (marked by C) and held at this temperature for 2.5 h (marked by D), the sample released another 6.4 wt % hydrogen, giving a total hydrogen amount of 16.8 wt %. This value is in good agreement with the TG result, thus further confirming the high purity of the hydrogen released from the AB/0.5Mg sample. Notably, the capacity gap between the delivered and the expected hydrogen amount from AB (16.8 vs ∼19 wt %) coincides with the capacity decrease in the first dehydrogenation step (3.7 vs ∼6 wt %). This seemingly implies a "capacity loss" from partial decomposition of AB in the milling process. But careful examination found no appreciable pressure build-up in the vial after mechanically milling. To better understand the apparent "capacity loss", we further preformed a designed TPD measurement, wherein the AB/0.5Mg sample was heated to 450 °C at a ramping rate of 0.5 °C/min. The TPD result (Figure S1, Supporting Information) showed that the desorbed hydrogen amount from AB reached up to ∼19 wt %, close to its theoretical value. This finding clearly indicates that the reduced hydrogen amount from the first dehydrogenation step does not come from the partial decomposition of AB in

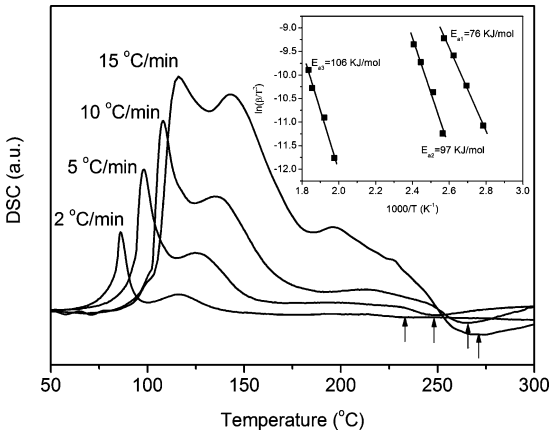

Figure 4. DSC profiles of the postmilled AB/0.5Mg samples at ramping rates of 2, 5, 10 °C/min, respectively. The inset presents the Kissinger plots for the three dehydrogenation steps. E_{a1}, E_{a2}, and E_{a3} are activation energies for the first, the second, and the third dehydrogenation steps, respectively. The arrows were added to indicate the peak temperatures of the third dehydrogenation step (i.e., ~233.2, 247.5, 266, and 271.3 °C from left to right).

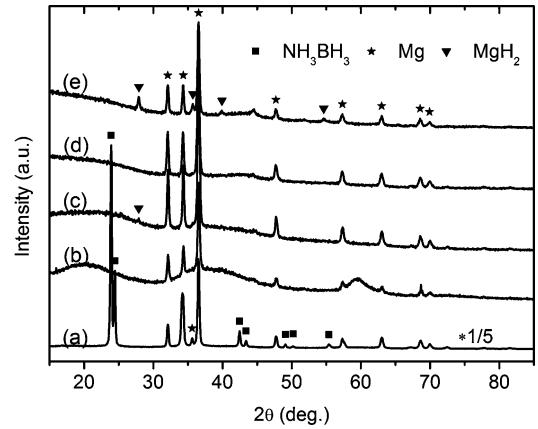

Figure 5. XRD patterns of the AB/0.5Mg sample in different stages: (a) after mechanically milling for 2 h; (b−d) quench-cooled to room temperature after being heated to 100, 200, 300 °C; and (e) held at 300 °C for 2.5 h after being heated to 300 °C (collected at A−D in Figure 3), respectively. For clarity, the intensity of the postmilled sample was multiplied by 1/5.

the milling process but may originate from the altered mechanistic pathway. In this regard, further detailed studies are still required.

As demonstrated above, the multistep dehydrogenation reaction of AB can be greatly promoted by mechanically milling with Mg. To gain insight into the improved kinetics, we determined the activation energy, E_a, of the individual dehydrogenation steps using the conventional Kissinger method.[37] Figure 4 presents the DSC profiles of the AB/0.5Mg sample at varied heating rates. Kissinger treatment of the heating rate-dependent peak temperature data yields a well-fitted line for each dehydrogenation step, as shown in the inset of Figure 4. From the slope of these straight lines, the activation energies for the first (E_{a1}), the second (E_{a2}), and the third (E_{a3}) dehydrogenation steps were determined to be 76, 97, 106 kJ/mol, respectively. The E_{a1} value for the AB/0.5Mg sample is much lower than that of pristine AB (~180 kJ/mol),[16,21] which is in good agreement with the observed kinetics enhancement, but the determined E_{a3} value is moderate, only slightly larger than E_{a2} for the second step. This is a questionable result because it was experimentally observed that the third dehydrogenation step is well-separated from the second one, with a peak temperature difference of >100 °C. Furthermore, the third dehydrogenation step is only slightly endothermic (as determined by combined TG/DSC analyses) and thereby fails to account for the high dehydrogenation temperature from a thermodynamic point of view. Combined analyses of these results suggest that the determined activation energy, E_{a3}, should deviate significantly from the truth value. One possible reason is that the third dehydrogenation step of the AB/0.5Mg sample may involve complicated multiple solid state reactions and cannot be appropriately described using the Kissinger model.

Phase/Structure/Chemical State Characterization. In our efforts to understand the pronounced promoting effect of Mg on the dehydrogenation reactions of AB, we performed combined phase/structure/chemical state analyses of the AB/0.5Mg sample in different stages. Figure 5 presents the XRD patterns of the postmilled AB/0.5Mg sample and its dehydrogenation products collected in different stages (points A−D of the TPD profile, as shown in Figure 3). In the postmilled sample, only the starting materials AB and Mg were identified. Careful examination of the XRD pattern found that the peak positions of both AB and Mg are essentially unchanged compared with those of the pristine phases, indicating that no solid phase reaction between AB and Mg occurs in the milling process. This is further evidenced by the lack of pressure build up in the vial after mechanical milling. After dehydrogenation at 100 °C (point A in Figure 3), the diffraction peaks of AB disappeared, and three broad and featureless peaks (centered at $2\theta = 20$, 39, and 59.5°, respectively) appeared, indicative of the formation of amorphous decomposition product(s). Of particular interest, comparison of the XRD patterns a and b found that the peak intensity of Mg was markedly reduced after the first dehydrogenation step. This is an important finding, showing clearly that a significant amount of Mg participates in the initial dehydrogenation reaction. In the subsequent heating process up to 200 °C (point B in Figure 3), a small amount of MgH_2 was formed, most probably via partial hydrogenation of the residual Mg, but upon further heating the sample to 300 °C (point C in Figure 3), the diffraction peaks of MgH_2 were found to disappear again (pattern d). These results clearly indicate that the in situ formed MgH_2 participates in the third dehydrogenation step. Finally, after the sample was held at 300 °C for 2.5 h, XRD examination clearly identified the residual Mg and the newly formed MgH_2. Here it should be noted that the XRD examination provides only the information of the crystalline phases. Judging from the significantly reduced peak intensity of the postheated sample relative to that of the postmilled sample, we speculated that a considerable amount of Mg has participated in the formation of amorphous decomposition products. This was strongly supported by the parallel FTIR analysis.

Figure 6 shows the FTIR spectra of the postmilled AB/0.5Mg sample and its dehydrogenated products in different stages. For comparison, the FTIR spectrum of the postmilled AB (for 2 h) was also included. The observed IR modes in the postmilled AB are in excellent agreement with the literature results,[28,33] indicating that mechanical milling alone exerts no appreciable influence on the bond structure of AB. But after mechanically milling with Mg, the B−N stretches of AB at 784 and 723 cm^{-1} were found to disappear largely. Interestingly, except for this notable change, we can identify no appreciable change of the N−H and B−H modes of AB. Because no solid phase reaction occurs in the milling process, the significantly weakened B−N stretching modes should be attributed to the solid interaction between AB and Mg. In this regard, sophisticated theoretical

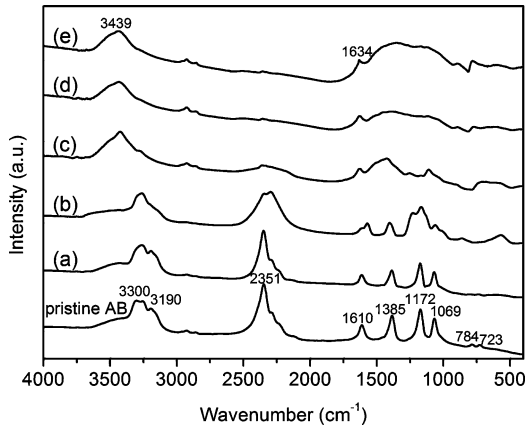

Figure 6. FTIR spectra of the AB/0.5Mg sample at varied states: (a) postmilled; (b−d) quench-cooled to room temperature after being heated to 100, 200, 300 °C; and (e) held at 300 °C for 2.5 h after being heated to 300 °C (collected at A−D in Figure 3), respectively. For comparison, pristine AB milled for 2 h was also presented. The broad peak centered at 3439 cm^{-1} and the peak at 1634 cm^{-1} should be assigned to O−H vibration, which originates from the moisture contamination of the samples.

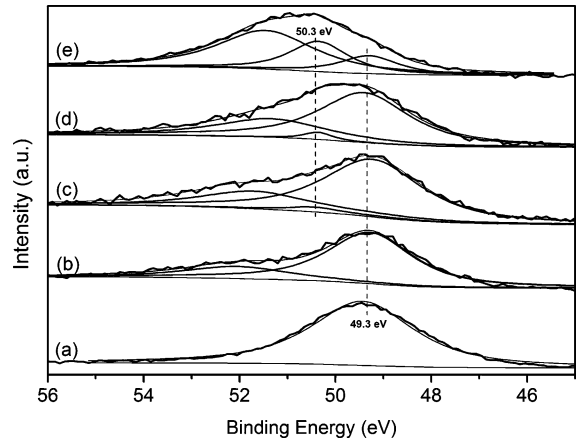

Figure 7. Comparison of Mg 2p photoelectron lines of the AB/0.5Mg sample at varied states: (a) postmilled; (b−d) quench-cooled to room temperature after being heated to 100, 200, 300 °C; and (e) held at 300 °C for 2.5 h after being heated to 300 °C (collected at A−D in Figure 3), respectively.

calculations may provide valuable hints to understand the effect of Mg on the electronic structure of AB. In the sample after dehydrogenation at 100 °C (pattern b), the identified N−H, B−H, and B−N modes evidenced the formation of $(NH_2BH_2)_n$ polymer. Additionally, the characteristic N−H bending and B−H torsion modes of $(NBH_x)_n$ polymer (the decomposition product of AB after releasing over one equivalent H_2) were also identified, which is indicative of the partial overlapping of the first two dehydrogenation step under the applied conditions. As the dehydrogenation reaction proceeds, the N−H and B−H bands were greatly weakened and finally disappeared in the sample after dehydrogenation at 300 °C (pattern d). This is in great contrast with the case of pristine AB, wherein the B−H and N−H stretches can be clearly identified after being heated to 300 °C (Figure S2, Supporting Information). These results are consistent with the property examination results, showing the promoting effect of Mg additive on the hydrogen release from AB. Interestingly, FTIR analysis of the postheated AB/0.5Mg sample at 300 °C could not identify the characteristic modes of BN (1370, 820 cm^{-1} for sp^2-bonded *h*-BN or *t*-BN, 1065 cm^{-1} for sp^3-bonded *c*-BN).[38] Instead, a broad band at 1000−1700 cm^{-1} and two weak modes at 889 and 779 cm^{-1} were observed in the dehydrogenation products. This result implies that the final products are not BN but probably Mg-containing complexes (i.e., Mg−N−B−H complexes).

In good agreement with the XRD and FTIR results, chemical state analysis by XPS also showed evidence of the participation of Mg in the dehydrogenation process of AB. As seen in Figure 7, the deconvoluted spectrum of the postheated sample at 100 °C clearly shows two peaks from chemically different Mg entities. The bonding state at 49.3 eV corresponds to elemental Mg, but the other one at higher energy side (52.1 eV) cannot be assigned to any known Mg-containing chemicals, including Mg nitride (Mg_3N_2, 50.5 eV)[39] and Mg boride (MgB_2, 49.5 eV).[40] The unknown chemical state of Mg was observed to gain intensity and slightly shifted to low-energy side with increasing dehydrogenation temperature, and ultimately it became the predominant chemical state of Mg in the sample after being held at 300 °C for 2.5 h (point D in Figure 3). Presumably, the unknown chemical state of Mg corresponds to the amorphous Mg−N−B−H species that are invisible in the XRD examinations. In that case, the slightly varied Mg 2p binding energies may originate from the composition/structure evolution of the decomposition products in the heating process. Additionally, the deconvoluted spectrum of the postheated sample at >200 °C also shows the signal of MgH_2 (50.3 eV). This is in general consistent with XRD results.

Solid-phase activation has recently been developed as a promising approach for preparation of AB-based hydrogen storage materials. Among the identified chemical promoters, Mg powder is the most cost-effective one. More importantly, the addition of Mg powder results in pronounced improvements of the dehydrogenation properties of AB on all key aspects: the enhanced dehydrogenation kinetics, the reduced induction period, the suppressed volatile byproduct, and the alleviated sample foaming, but similar to other AB-based materials, the AB/Mg system lacks facile reversibility. Whereas the exothermicity of the dehydrogenation reaction of AB had been significantly reduced and even tailored to be endothermic for the third dehydrogenation step by adding Mg, it appears unrealistic to anticipate the hydride restoration via solid−gas reaction. Another weakness of the AB/Mg system is the capacity loss arising upon the addition of Mg. For example, the deliverable hydrogen capacity of the AB/0.5Mg system is ∼30% lower than that of AB, but our preliminary study found that the sample with lower Mg addition amount but longer milling time could behave similarly to the AB/0.5Mg sample. This finding showed the potential of nanoengineering approach in solving the capacity loss problem. Finally, the mechanism underlying the promoting effect of Mg on the dehydrogenation reactions of AB is still unclear. In a closely relevant study, we found that mechanically milling with MgH_2 can remarkably improve the dehydrogenation property of AB to a similar extent as the present AB/Mg system, but combined phase/structural characterizations showed that at least in the early stages Mg exerts its promoting effect by directly interacting with AB without experiencing the MgH_2 intermediate. This finding indicates that Mg may differ substantially from MgH_2 in terms of promoting mechanism.

Conclusions

Hydrogen release from AB can be greatly promoted by mechanically milling with commercial Mg powder. The postmilled AB/0.5Mg sample can release ca. 8.2 wt % hydrogen at 100 °C with an average dehydrogenation rate five times faster

than that of pristine AB. Upon elevating the dehydrogenation temperature to 300 °C, >2.5 equiv hydrogen can be released from AB, giving a material-based hydrogen capacity of 12 wt %. Additionally, mechanically milling with Mg powder has proven to be an effective approach for alleviating sample foaming and for tailoring the thermochemical property of AB. Combined phase/structure/chemical state analyses showed that considerable amount of Mg participates in the dehydrogenation process, resulting in the formation of Mg−N−B−H product(s). Furthermore, our study results suggested that at least in the early stages, Mg may exert its promoting effect via directly interacting with the host AB rather than experiencing the MgH_2 intermediate. Mg is an elemental reactant that has been proven to be effective for promoting the dehydrogenation properties of AB. Better understanding of the promoting effect of Mg and the reaction mechanistic pathway of the AB/Mg system may aid the design and synthesis of novel B−N compounds for chemical hydrogen storage.

Acknowledgment. The financial supports from the National Natural Science Foundation of China (grant nos. 50771094 and 50801059), the National High-Tech R&D Program of China (863 Program, grant no. 2009AA05Z109), the National Program on Key Basic Research Project (973 Program, grant no. 2010CB631305), the Frontier Project of CAS Knowledge Innovation Program (no. KGCXZ-YW-342), and the special funding for CAS President Prize winner are gratefully acknowledged.

Supporting Information Available: Elemental analysis result of the synthesized AB, the temperature-programmed desorption profile of the AB/0.5Mg sample up to 450 °C, and the FTIR spectrum of pristine AB after being heated at 300 °C. This material is available free of charge via the Internet at http://pubs.acs.org.

References and Notes

(1) Schlapbach, L.; Züttel, A. *Nature* **2001**, *414*, 353.
(2) Grochala, W.; Edwards, P. P. *Chem. Rev.* **2004**, *104*, 1283.
(3) Orimo, S.; Nakamori, Y.; Eliseo, J. R.; Züttel, A.; Jensen, C. M. *Chem. Rev.* **2007**, *107*, 4111.
(4) Marder, T. B. *Angew. Chem., Int. Ed.* **2007**, *46*, 8116.
(5) Stephens, F. H.; Pons, V.; Baker, R. T. *Dalton Trans.* **2007**, *25*, 2613.
(6) Wang, P.; Kang, X. D. *Dalton Trans.* **2008**, *40*, 5400.
(7) Jaska, C. A.; Temple, K.; Lough, A. J.; Manners, I. *J. Am. Chem. Soc.* **2003**, *125*, 9424.
(8) Denney, M. C.; Pons, V.; Hebden, T. J.; Heinekey, D. M.; Goldberg, K. I. *J. Am. Chem. Soc.* **2006**, *128*, 12048.
(9) Blaquiere, N.; Diallo-Garcia, S.; Gorelsky, S. I.; Black, D. A.; Fagnou, K. *J. Am. Chem. Soc.* **2008**, *130*, 14034.
(10) Keaton, R. J.; Blacquiere, J. M.; Baker, R. T. *J. Am. Chem. Soc.* **2007**, *129*, 1844.
(11) Stephens, F. H.; Baker, R. T.; Matus, M. H.; Grant, D. J.; Dixon, D. A. *Angew. Chem., Int. Ed.* **2007**, *46*, 746.
(12) Bluhm, M. E.; Bradley, M. G.; Butterick III, R.; Kusari, U.; Sneddon, L. G. *J. Am. Chem. Soc.* **2006**, *128*, 7748.
(13) Cheng, F. Y.; Ma, H.; Li, Y. M.; Chen, J. *Inorg. Chem.* **2007**, *46*, 788.
(14) Dai, H. B.; Gao, L. L.; Liang, Y.; Kang, X. D.; Wang, P. *J. Power Sources* **2010**, *195*, 307.
(15) Chandra, M.; Xu, Q. *J. Power Sources* **2006**, *159*, 855.
(16) Gutowska, A.; Li, L. Y.; Shin, Y.; Wang, C. M.; Li, X. S.; Linehan, J. C.; Smith, R. S.; Kay, B. D.; Schmid, B.; Shaw, W.; Gutowski, M.; Autrey, T. *Angew. Chem., Int. Ed.* **2005**, *44*, 3578.
(17) Feaver, A.; Sepehri, S.; Shamberger, P.; Stowe, A.; Autrey, T.; Cao, G. Z. *J. Phys. Chem. B* **2007**, *111*, 7469.
(18) Li, L.; Yao, X. D.; Sun, C. H.; Du, A. J.; Cheng, L. N.; Zhu, Z. H.; Yu, C. Z.; Zou, J.; Smith, S. C.; Wang, P.; Cheng, H. M.; Frost, R. L.; Lu, G. Q. *Adv. Funct. Mater.* **2009**, *19*, 265.
(19) Zhao, J. Z.; Shi, J. F.; Zhang, X. W.; Cheng, F. Y.; Liang, J.; Tao, Z. L.; Chen, J. *Adv. Mater.* **2010**, *22*, 394.
(20) Xiong, Z. T.; Yong, C. K.; Wu, G. T.; Chen, P.; Shaw, W.; Karkamkar, A.; Autrey, T.; Jones, M. O.; Johnson, S. R.; Edwards, P. P.; David, W. I. F. *Nat. Mater.* **2008**, *7*, 138.
(21) Kang, X. D.; Fang, Z. Z.; Kong, L. Y.; Cheng, H. M.; Yao, X. D.; Lu, G. Q.; Wang, P. *Adv. Mater.* **2008**, *20*, 2756.
(22) Xiong, Z. T.; Wu, G. T.; Chua, Y. S.; Hu, J. J.; He, T.; Xu, W. L.; Chen, P. *Energy Environ. Sci.* **2008**, *1*, 360.
(23) Diyabalanage, H. V. K.; Shrestha, R. P.; Semelsberger, T. A.; Scott, B. L.; Bowden, M. E.; Davis, B. L.; Burrell, A. K. *Angew. Chem., Int. Ed.* **2007**, *46*, 8995.
(24) Wu, H.; Zhou, W.; Yildirim, T. *J. Am. Chem. Soc.* **2008**, *130*, 14834.
(25) Zhang, Q. A.; Tang, C. X.; Fang, C. H.; Fang, F.; Sun, D. L.; Ouyang, L. Z.; Zhu, M. *J. Phys. Chem. C* **2010**, *114*, 1709.
(26) Kang, X. D.; Ma, L. P.; Fang, Z. Z.; Gao, L. L.; Luo, J. H.; Wang, S. C.; Wang, P. *Phys. Chem. Chem. Phys.* **2009**, *11*, 2507.
(27) Neiner, D.; Karkamkar, A.; Linehan, J. C.; Arey, B.; Autrey, T.; Kauzlarich, S. M. *J. Phys. Chem. C* **2009**, *113*, 1098.
(28) Hu, M. G.; Paasschen, J. M. V.; Geanangel, R. A. *J. Inorg. Nucl. Chem.* **1977**, *39*, 2147.
(29) Hu, M. G.; Geanangel, R. A.; Wendlandt, W. W. *Thermochim. Acta* **1978**, *23*, 249.
(30) Sit, V.; Geanangel, R. A.; Wendlandt, W. W. *Thermochim. Acta* **1987**, *113*, 379.
(31) Wolf, G.; Baumann, J.; Baitalow, F.; Hoffmann, F. P. *Thermochim. Acta* **2000**, *343*, 19.
(32) Baitalow, F.; Baumann, J.; Wolf, G.; Jaenicke-Rőβler, K.; Leitner, G. *Thermochim. Acta* **2002**, *391*, 159.
(33) Baumann, J.; Baitalow, F.; Wolf, G. *Thermochim. Acta* **2005**, *430*, 9.
(34) He, T.; Xiong, Z. T.; Wu, G. T.; Chu, H. L.; Wu, C. Z.; Zhang, T.; Chen, P. *Chem. Mater.* **2009**, *21*, 2315.
(35) Kalidindi, S. B.; Joseph, J.; Jagirdar, B. R. *Energy Environ. Sci.* **2009**, *2*, 1274.
(36) Heldebrant, D. J.; Karkamkar, A.; Hess, N. J.; Bowden, M.; Rassat, S.; Zheng, F.; Rappe, K.; Autrey, T. *Chem. Mater.* **2008**, *20*, 5332.
(37) Kissinger, H. E. *Anal. Chem.* **1957**, *29*, 1702.
(38) Friedmann, T. A.; Mirkarimi, P. B.; Medlin, D. L.; McCarty, K. F.; Klaus, E. J.; Boehme, D. R.; Johnsen, H. A.; Mills, M. J.; Ottesen, D. K.; Barbour, J. C. *J. Appl. Phys.* **1994**, *76*, 3088.
(39) Soto, G.; Díaz, J. A.; Cruz, W. D. L.; Reyes, A.; Samano, E. C. *J. Non-Cryst. Solids* **2004**, *342*, 65.
(40) Aswal, D. K.; Muthe, K. P.; Singh, A.; Sen, S.; Shah, K.; Gupta, L. C.; Gupta, S. K.; Sahni, V. C. *Physica C* **2001**, *363*, 208.

JP911931T